Inorganica Chimica Acta 367 (2011) 187–193

Contents lists available at ScienceDirect

Inorganica Chimica Acta

journal homepage: www.elsevier.com/locate/ica

Four new coordination polymers involving transition metals with 1,2,4,5-benzenetetracarboxylate and pyridyl-donor ligand di(4-pyridyl) sulfide

Charlane C. Corrêa [a], Lívia B. Lopes [a], Leonardo H.R. dos Santos [a], Renata Diniz [a], Maria I. Yoshida [b], Luiz F.C. de Oliveira [a], Flávia C. Machado [a,*]

[a] Núcleo de Espectroscopia Estrutura Molecular, Departamento de Química, Universidade Federal de Juiz de Fora, Campus Universitário s/n, Martelos, Juiz de Fora, MG 36036-900, Brazil

[b] Departamento de Química, Universidade Federal de Minas Gerais, Pampulha, Belo Horizonte, MG 31270-901, Brazil

ARTICLE INFO

Article history:
Received 30 July 2010
Received in revised form 10 December 2010
Accepted 13 December 2010
Available online 23 December 2010

Keywords:
Coordination polymers
Transition metal
Di(4-pyridyl) sulfide
1,2,4,5-Benzenetetracarboxylate
Crystal structure

ABSTRACT

Four new coordination polymers namely $\{[Mn_2(BT)(DPS)_2(H_2O)_6]\cdot 10H_2O\}_n$ (**MnBTDPS**), $\{[Co_2(BT)(DPS)_2(H_2O)_6]\cdot 10H_2O\}_n$ (**CoBTDPS**), $\{[Cu_2(BT)(DPS)(H_2O)_4]\cdot 5H_2O\}_n$ (**CuBTDPS**) and $\{[Zn_2(BT)(DPS)_2]\cdot 6H_2O\}_n$ (**ZnBTDPS**), where BT = 1,2,4,5-benzenetetracarboxylate and DPS = di(4-pyridyl) sulfide, were synthesized and characterized by thermal analysis, vibrational spectroscopy (Raman and infrared) and single crystal X-ray diffraction analysis. In all compounds, the DPS ligands are coordinated to metal sites in a bridging mode and the carboxylate moiety of BT ligands adopts a monodentate coordination mode, as indicated by the Raman spectra data through the $\Delta\nu$ ($\nu_{asym}(COO) - \nu_{sym}(COO)$) value. According to X-ray diffraction analysis, **MnBTDPS** and **CoBTDPS** are isostructural and in these cases, the metal centers exhibit a distorted octahedral geometry. In **CuBTBPP**, the Cu^{2+} centers geometries are best described as square-pyramids, according to the trigonality index $\tau = 0.14$ for Cu1 and $\tau = 0.10$ for Cu2. On the other hand, in **ZnBTDPS**, the Zn^{2+} sites adopt a tetrahedral geometry. Finally, the four compounds formed two-dimensional sheets that are connected to each other through hydrogen bonding giving rise to three-dimensional supramolecular arrays.

1. Introduction

The supramolecular chemistry is one of the most promising areas of research in chemistry [1], because of the wide variety of compounds structural topologies and their various applications as optic, electronic and magnetic devices or microporous materials [2–4]. Recent studies show the complexity in the construction of metal–organic networks [5]. Among the factors that affect the final structure topology, we can cite the organic ligands conformations and their coordination ability, the metal center geometries, the solvent polarity and the reaction medium pH conditions [6,7].

Organic aromatic polycarboxylate ligands have been extensively employed in the preparation of such metal–organic compounds with multidimensional networks [8]. In this aspect, 1,2,4,5-benzenetetracarboxylate (BT), known as pyromellitato anion, is a good candidate for the construction of novel metal–organic hybrid compounds since eight O-donor atoms are available for coordination, generating various and sometimes surprising molecular architectures [9–14]. Furthermore, carboxylate ligands exhibit a versatile coordination behavior, including bridging coordination modes that provide exchange-coupling pathways when paramagnetic metals are involved [15]. Several pyromellitato complexes with various transition metals have been reported in the literature [16,14,13,17], mainly combined with nitrogen ligands such as 2,2′-bipyridine and 4,4′-bipyridine [18–24]. There are also examples of pyromellitato complexes with lanthanide ions [25].

The introduction of bidentate N-ligands in the system may lead to new structural evolution, adjusting these metal–organic hybrid compounds dimensionality [8]. The di(4-pyridyl) sulfide (DPS) ligand is essentially bent around the sulfur atom (C–S–C, 100°) presenting some flexibility in contrast to linear rigid ligands such as 4,4′-bipyridine [26]. DPS ligand can act in the bridging coordination mode and has been exploited to produce a number of new coordination polymers [27,5,28–31]. However, it is important to mention that 3D coordination polymers containing DPS ligands are very rare [30].

In this work, we report the synthesis, spectroscopic properties and crystal structures of four new compounds of Mn^{2+}, Co^{2+}, Cu^{2+} and Zn^{2+} all containing the nitrogen ligand DPS and the polycarboxylate anion 1,2,4,5-benzenetetracarboxylate (pyromellitate anion).

* Corresponding author. Tel.: +55 32 2102 3310; fax: +55 32 2102 3314.
E-mail address: flavia.machado@ufjf.edu.br (F.C. Machado).

0020-1693
doi:10.1016/j.ica.2010.12.034

2. Experimental

2.1. Materials and methods

The di(4-pyridyl)sulfide (DPS) ligand can be obtained according to the published method [32], however, it was synthesized following the procedure adopted for di(2-pyridyl)sulfide (2-DPS) ligand [33]. A mixture of 4-mercaptopyridine (2.5 g, 22 mmol), 4-bromo-pyridine (4.3 g, 0.22 mmol) and potassium carbonate (4 g) in dimethylformamide (15 mL) was heated under reflux for 48 h. After cooling, the solvent was removed by rotary evaporation. The yellow solid was obtained after extraction using dichloromethane:water solvent mixture. Yield: 3.93 g, 94%. Mp 68–69 °C.

All solvents and reagents were commercially available, purchased from Aldrich® and used without further purification. Elemental analyses for C, H and N were carried out on a Perkin-Elmer 2400 analyzer. Infrared spectra were recorded on a FT-IR Bomen MB102 spectrometer in the frequency range 4000–400 cm^{-1} with an average of 128 scans and 4 cm^{-1} of spectral resolution using KBr pellets. Fourier-transform Raman spectroscopy was carried out using a Brucker RFS 100 instrument equipped with an Nd^{3+}/YAG laser operating at 1064 nm in the near infrared and a CCD detector cooled with liquid nitrogen with an average of 1000 scans and 4 cm^{-1} of spectral resolution. Thermal analysis (TG/DTA) data were collected on a Shimadzu TG-60 using 3.0 mg packed in alumina crucible. Samples were heated at 10 °C/min from room temperature to 800 °C in a dynamic nitrogen atmosphere (flow rate = 100 mL/min).

2.2. Synthesis of the compounds

An ethanolic solution of H_4BT (70 mg, 0.26 mmol) was neutralized by addition of an aqueous solution Na_2CO_3 (58.42 mg, 0.52 mmol) and stirred for 20 min. Then, an ethanolic solution of DPS (52 mg, 0.26 mmol) was added. After that, an aqueous solution of the appropriate hydrated metal chloride (0.26 mmol in the 10 mL of water) was added by slow diffusion. In all cases, colored solids precipitated and were filtered off. The resulting solutions were set aside and after one week single crystals were collected and analyzed by thermal analysis, vibrational spectroscopy and X-ray diffraction techniques.

2.2.1. $\{[Mn_2(BT)(DPS)_2(H_2O)_6]\cdot 10H_2O\}_n$ (MnBTDPS)

Color: yellow. Yield: 42%. *Anal.* Calc. for $Mn_2C_{30}O_{24}H_{50}N_4S_2$: C, 35.16; H, 4.92; N, 5.47%. Found: C, 35.31; H, 4.82; N, 5.54%. IR (KBr, cm^{-1}): 3417(F), 1615(F), 1590(F), 1582(F), 1546(F), 1482(F), 1416(F), 1368(F), 1317(m), 1249(m), 1222(m), 1182(f), 1106(m), 1067(m), 1008(m), 829(F), 724(F). Raman (1064 nm, cm^{-1}): 3070(F), 1610(o), 1592(F), 1550(m), 1487(f), 1429(m), 1382(mf), 1324(f), 1230(m), 1173(F), 1115(F), 1068(m), 1015(mF), 821(f), 727(f), 669(f).

2.2.2. $\{[Co_2(BT)(DPS)_2(H_2O)_6]\cdot 10H_2O\}_n$ (CoBTDPS)

Color: pink. Yield: 35%. *Anal.* Calc. for $Co_2C_{30}O_{24}H_{50}N_4S_2$: C, 35.51; H, 4.77; N, 5.52%. Found: C, 35.32; H, 4.72; N, 5.53%. IR (KBr, cm^{-1}): 3385(F), 1601(o), 1590(F), 1559(F), 1485(F), 1420(F), 1378(F), 1328(F), 1224(m), 1176(mf), 1135(m), 1106(m), 1018(m), 817(F), 725(F). Raman (1064 nm, cm^{-1}): 3070(F), 1602(F), 1589(F), 1547(f), 1492(f), 1432(m), 1373(f), 1323(F), 1232(m), 1187(f), 1121(F), 1068(m), 1015(F), 829(f), 721(f), 663(f).

2.2.3. $\{[Cu_2(BT)(DPS)(H_2O)_4]\cdot 5H_2O\}_n$ (CuBTDPS)

Color: blue. Yield: a small amount. *Anal.* Calc. for $Cu_2C_{20}O_{17}H_{28}N_2S$: C, 33.01; H, 3.88; N, 3.85%. Found: C, 34.05; H, 3.76; N, 3.81%. IR (KBr, cm^{-1}): 3424(F), 1615(F), 1591(F), 1553(F), 1491(F), 1419(F), 1371(F), 1330(F), 1223(f), 1189(f), 1110(f), 1065(f), 1028(f), 818(m), 730(m). Raman (1064 nm, cm^{-1}): 3080(F), 3070(F), 1614(o), 1597(o), 1557(f), 1482(f), 1422(m), 1360(f), 1325(mF), 1228(m), 1186(m), 1116(F), 1067(m), 1027(F), 830(F), 732(f), 662(m).

2.2.4. $\{[Zn_2(BT)(DPS)_2]\cdot 6H_2O\}_n$ (ZnBTDPS)

Color: colorless. Yield: 38%. *Anal.* Calc. for $Zn_2C_{30}O_{14}H_{30}N_4S_2$: C, 41.63; H, 3.49; N, 6.47%. Found: C, 41.65; H, 3.17; N, 5.91%. IR (KBr, cm^{-1}): 3434(F), 3095(F), 1618(F), 1597(o), 1555(m), 1492(f), 1431(m), 1384(F), 1328(F), 1234(F), 1174(F), 1116(F), 1070(m), 1034(F), 822(m), 733(F). Raman (1064 nm, cm^{-1}): 3066(F), 3091(F), 1634(o), 1598(F), 1547(f), 1496(f), 1411(m), 1356(mf), 1339(f), 1237(m), 1181(f), 1126(F), 1069(F), 1030(mF), 828(f), 740(m), 664(m).

2.3. X-ray diffraction

Single crystal X-ray data of all compounds were collected using a Bruker Kappa CCD diffractometer with Mo Kα (λ = 0.71073 Å) at room temperature. Data collection, reduction and cell refinement were performed by COLLECT [34], EVALCCD [35] and DIRAX [36] programs, respectively. The structures were solved and refined using SHELXL-97 [37]. An empirical isotropic extinction parameter *x* was refined, according to the method described by Larson [38]. A multiscan absorption correction was applied [39]. Anisotropic displacement parameters were assigned to all non-hydrogen atoms. Hydrogen atoms were located from Fourier difference maps and isotropic displacement parameters were refined in group. The structures were drawn by ORTEP-3 for Windows [40] and Mercury [41] programs.

3. Results and discussion

The metallic complexes, hereafter named MBTDPS, where M = Mn^{2+}, Co^{2+}, Cu^{2+} and Zn^{2+}, were obtained by the diffusion of the respective metal chloride aqueous solution into an ethanolic solution containing both DPS and BT ligands. The analytical data suggest the stoichiometric ratios as (2:1:2)/(M:BT:DPS), for M = Mn^{2+}, Co^{2+} and Zn^{2+}, and (2:1:1)/ (M:BT:DPS) for copper compound.

Thermal analysis data of four compounds have been deposited as Supplementary material (Fig. S1). In the TG curve of all compounds, a first mass loss between 32 and 100 °C is observed and was attributed to the release of water molecules. In **MnBTDPS** curve, this loss corresponds to 12 H_2O (Obsd., 20.29%; Calc., 21.09%), in **CoBTDPS** to 4 H_2O (Obsd., 7.14%; Calc., 7.10%), in **CuBTDPS** to 7 H_2O (Obsd., 17.37%; Calc., 17.32%) and in **ZnBTDPS** to 6 H_2O (Obsd., 13.03%; Calc., 12.48%). These dehydration paths were identified in the DTA curves by endothermic events at 75, 38, 55 and 47 °C for **MnBTDPS**, **CoBTDPS**, **CuBTDPS** and **ZnBTDPS**, respectively.

Above 150 °C, four mass losses were identified in the curve of **MnBTDPS**, being attributed to other four water molecules release and to organic ligands partial decomposition. At 750 °C, the high percentage final residue of 43.27%, indicates the incomplete thermal decomposition up to this temperature. **CoBTDPS** TG curve presents a second mass loss in the 41–100 °C temperature range that corresponds to another dehydration path with the release of 10 H_2O (Obsd., 17.87%; Calc., 17.75%). This path was identified in the DTA curve as an endothermic event at 86 °C. Above 200 °C, the decomposition of the organic constituents takes place and at 750 °C the final residue of 17.95% probably contains 2 mol of CoO along with some carbonized material. In **CuBTDPS** and **ZnBTDPS** TG curves, after the dehydration paths, stability plateaus are

observed up to 300 °C and above this temperature, the decomposition of organic ligands occurs in both cases.

Vibrational spectra of the compounds **MBTDPS** and the main vibrational modes were deposited as Supplementary material (Table S1) and are in agreement with crystal data. The infrared spectra of the compounds **MBTDPS** show a broad band around 3400 cm^{-1} assigned to ν_{OH}, indicating that all compounds present water molecules in their structures, in accordance to the thermal analysis results. Also, they exhibit similar characteristics with regard to the $\nu_{CC/CN}$ pyridine ring stretching modes of DPS ligand. In all cases, the main pyridine ring vibrational bands shift from 1568 cm^{-1} and 1478 cm^{-1} in free DPS to about 1590 and 1490 cm^{-1}. In fact, the presence of $\nu_{CC/CN}$ at higher wavernumbers in complexes is indicative of metal coordination to DPS pyridine nitrogen atoms, as observed for other compounds containing pyridine derivative ligands described in the literature [5,42–48].

The most interesting aspect of the Raman spectra of these compounds is concerned to the bands related to asymmetric and symmetric stretching modes of COO groups from the carboxylate ligands. For these compounds, these bands appear at approximately 1610 and 1230 cm^{-1}, respectively. In this class of compounds, the difference between ν_{asym}(COO) and ν_{sym}(COO) ($\Delta\nu$) in comparison to the corresponding values in ionic species is currently employed to determine a characteristic carboxylate group coordination mode [49,50]. In the Raman spectrum of the sodium 1,2,4,5-benzenetetracarboxylate (Na_4BT) the ν_{asym}(COO) and ν_{sym}(COO) are, respectively, 1605 and 1440 cm^{-1} ($\Delta\nu$ = 165 cm^{-1}). For the four complexes, these values are larger than the one of the sodium salt, **MnBTDPS** ($\Delta\nu$ = 380 cm^{-1}); **CoBTDPS** ($\Delta\nu$ = 370 cm^{-1}); **CuBTDPS** ($\Delta\nu$ = 386 cm^{-1}) and **ZnBTDPS** ($\Delta\nu$ = 397 cm^{-1}) indicating that in all complexes the carboxylate group is coordinated to the metal center in a monodentate fashion.

3.1. Crystal structures

The polymeric nature of compounds **MBTDPS** was revealed by single crystal X-ray diffraction structural analysis. Table 1 exhibits crystal data and Tables S2–S5, the main geometrical parameters of the four complexes.

3.2. $\{[Mn_2(BT)(DPS)_2(H_2O)_6]\cdot 10H_2O\}_n$ (**MnBTDPS**) and $\{[Co_2(BT)(DPS)_2(H_2O)_6]\cdot 10H_2O\}_n$ (**CoBTDPS**)

Comparing the listed crystallographic parameters (Table 1), it can be noticed that compounds **MnBTDPS** and **CoBTDPS** are isostructural. Fig. 1 presents part of the crystalline structure of these compounds elucidating the coordination spheres of two crystallographically independent metal centers. Both metals adopt a distorted octahedral geometry with the core MO_4N_2 in a *trans* arrangement. The M1 atom is coordinated to two oxygen atoms O1 and $O1^i$ from the carboxylate group, two oxygen atoms O5 and $O5^i$ from water molecules and two nitrogen atoms N1 and $N1^i$ from DPS ligand [symmetry codes: $i(-x, 1-y, 1-z)$]. The M2 atom is coordinated to four oxygen atoms O6, $O6^{iv}$, O7 and $O7^{iv}$ from water molecules and two nitrogen atoms N2 and $N2^{iv}$ from DPS ligand [symmetry codes: $iv(-1-x, 3-y, -z)$]. As can be seen in Fig. 1, the metal sites M1 and M2 are located in inversion center of the structure. The M–O and M–N bond distances and some selected bond angles are displayed in Tables S2 and S3 and it can be noticed that M–N bonds are longer than M–O ones.

Two carboxylate groups of BT ligands are coordinated to the metal centers in a monodentate mode, as indicated by vibrational spectroscopy results, and BT ligands are connecting M1 atoms along the crystallographic *b*-axis with M1···M1 distance of 11.3083 (5) Å for **MnBTDPS** and 11.154 (5) Å for **CoBTDPS**. DPS ligands act in a bridging mode connecting M1 and M2 sites with M1···M2 distances of 11.027 (8) and 10.948 (10) Å for manganese and cobalt compounds, respectively. These connections lead to closed paths of approximately 11 × 22 Å dimension, formed by six metals (four M1 and two M2), two BT ligands and four DPS ligands, giving rise to 2D rhombohedral sheets as shown in Fig. 2.

Considering the metals M1 and M2 as nodes and using program package TOPOS [51], the network of these compounds can be

Table 1
Crystal data of **MBTDPS** compounds.

Compound	MnBTDPS	CoBTDPS	CuBTDPS	ZnBTDPS
Formula	$C_{30}H_{50}Mn_2N_4O_{24}S_2$	$C_{30}H_{50}Co_2N_4O_{24}S_2$	$C_{20}H_{28}Cu_2N_2O_{17}S$	$C_{30}H_{30}Zn_2N_4O_{14}S_2$
Formula weight (g mol^{-1})	1024.74	1032.72	727.5	865.44
Crystal system	triclinic	triclinic	monoclinic	triclinic
Space group	$P\bar{1}$	$P\bar{1}$	$P2_1/n$	$P\bar{1}$
Unit cell dimensions				
a (Å)	10.125(9)	9.917(10)	13.692 (3)	8.967(5)
b (Å)	11.308(5)	11.154(5)	12.039(2)	9.318(7)
c (Å)	11.788(9)	11.723(8)	16.888 (3)	10.813(10)
α (°)	63.338(5)	63.990(4)	90.00	76.910(6)
β (°)	77.670(7)	78.250(10)	90.01(3)	73.410(6)
γ (°)	80.150(6)	80.630(8)	90.00	75.280(5)
V ($Å^3$)	1173.95(15)	1137.0(15)	2783.7(10)	825.90(11)
Z	1	1	1	1
Crystal size (mm)	0.27 × 0.16 × 0.08	0.26 × 0.14 × 0.02	0.44 × 0.18 × 0.13	0.22 × 0.17 × 0.04
d_{calc} (g cm^{-3})	1.449	1.508	0.847	1.740
μ(Mo Kα) (cm^{-1})	0.710	0.9074	0.829	1.657
T_{min}/T_{max}	0.6193/0.9415	0.8248/0.9081	0.6479/0.8184	0.6961/0.9389
Measured reflections	15,649	13,862	18,045	10,159
Unique reflections	5302	5146	5934	3725
Observed reflections[a]	3332	3714	4628	2559
No. parameters	292	300	383	236
R[b]	0.0517	0.0465	0.0427	0.0526
wR[a]	0.0989	0.1094	0.1182	0.1081
S	1.041	1.022	1.444	1.039
RMS peak (e $Å^{-3}$)	0.069	0.073	0.093	0.107

[a] $[F_o^2 > 2\sigma(F_o^2)]$.
[b] $[F_o > 2\sigma(F_o)]$.

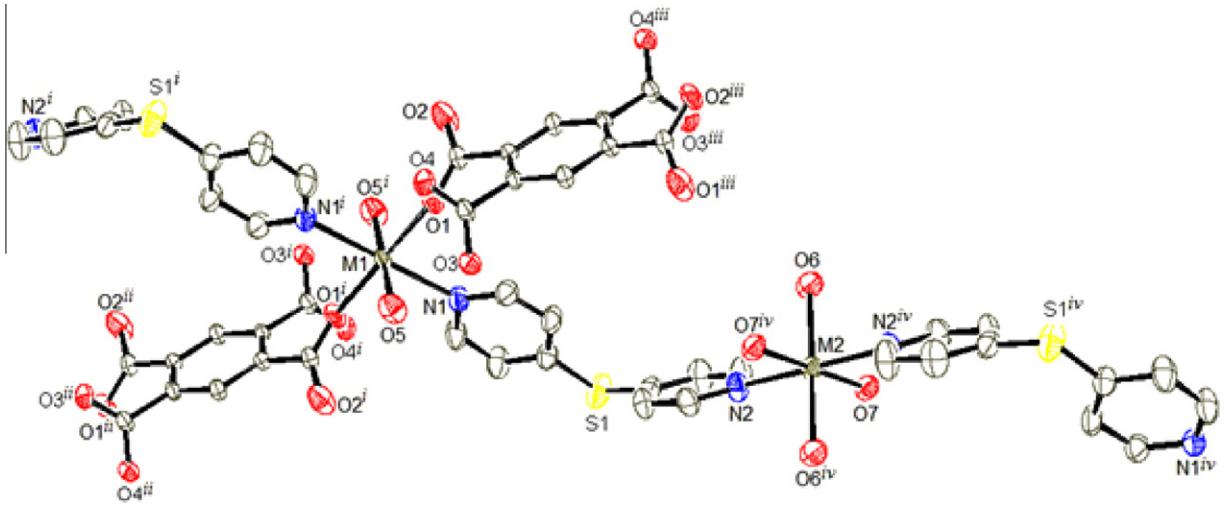

Fig. 1. Crystal structure of compounds **MnBTDPS** and **CoBTDPS**. Symmetry codes: *i*(−*x*, 1 − *y*, 1 − *z*); *ii*(*x*, −1 + *y*, *z*); *iii*(−*x*, 2 − *y*, 1−*z*) and *iv*(−1 − *x*, 3 − *y*, −*z*). The hydrogen atoms and the lattice water molecules have been omitted for clarity.

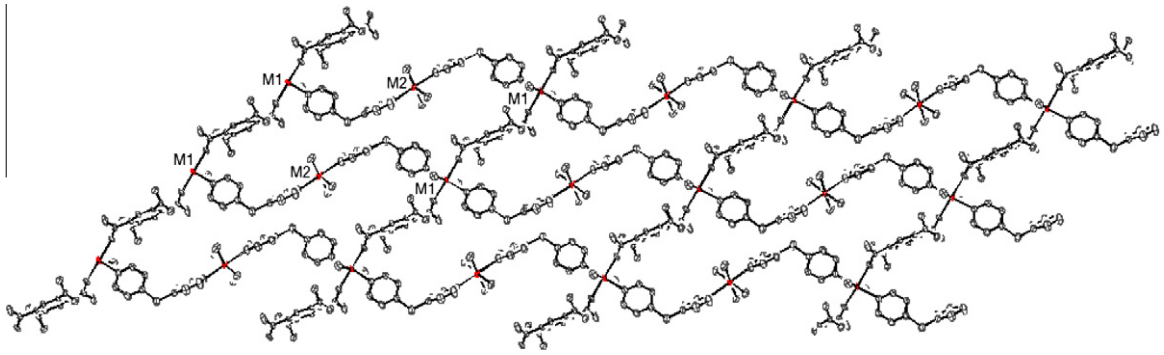

Fig. 2. 2D arrangement of compounds **MnBTDPS** and **CoBTDPS**.

described as a bi-nodal 4,2-connected network with short Schläfli symbols (6^4 8 10)(6) for M1 and M2, respectively.

One two-dimensional sheet interacts with other parallel sheets through O–H···O hydrogen bonds between oxygen atoms from coordinated water molecules of one sheet and free oxygen atoms from carboxylate groups of adjacent sheets generating a three-dimensional arrangement. The geometric parameters of hydrogen bonds observed in these compounds are listed in Tables S2 and S3.

3.3. $[Cu_2(BT)(DPS)(H_2O)_4]\cdot 5H_2O\}_n$ (CuBTDPS)

Fig. 3 shows a structural fragment of compound **CuBTDPS**. It can be noticed two crystallographically independent Cu^{2+} centers. Cu1 is coordinated by five oxygen atoms being three from water molecules (O9, O10 and O11) and two from a carboxylate group (O1 and O6). Cu2 is also penta-coordinated by three oxygen atoms being two from carboxylate groups (O4 and O7) and one from a water molecule (O12) and by two nitrogen atoms (N1 an $N1^i$) from the DPS ligand. In this compound, the trigonality index [52] values τ are 0.14 and 0.10 for Cu1 and Cu2, respectively, indicating that both sites geometry is best described as slightly distorted square-pyramid. Table S4 exhibits some selected bond distances and angles for **CuBTDPS**. For Cu1, the basal plane is formed by O1, O6, O10 and O11 and the apical position is occupied by O9 atom and for Cu2, and the basal plane is formed by O4, O7, N1 and $N1^i$ while the apical position is occupied by O12 atom. Cu1–O9 and Cu2–O12 bond distances are much longer than any other Cu–O or Cu–N distances, characterizing the presence of Jahn–Teller effect. BT ligands carboxylate groups are coordinated in a monodentate mode, as suggested by vibrational spectroscopy data. In this case, it can be noticed that C–O bond distances, in which the oxygen atom is

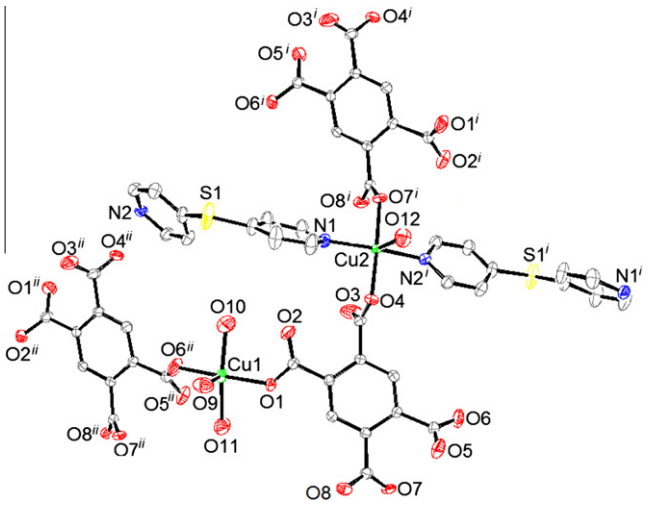

Fig. 3. ORTEP view of structural fragment of compound **CuBTDPS**. The hydrogen atoms and the lattice water molecules have been omitted for clarity; [symmetry codes: *i*(−0.5 + *x*, 1.5 − *y*, 0.5 + *z*) and *ii*(0.5 + *x*, 1.5 − *y*, 0.5 + *z*)].

coordinated to the metal center (C7–O1, 1.256(4); C8–O4, 1.258(4); C9–O6, 1.256(4) and C10–O7, 1.259(4) Å) are longer than the C–O bond distances in which the oxygen atom is free (C7–O2, 1.226(4); C8–O3, 1.222(4); C9–O5, 1.225(4) and C10–O8, 1.240(4) Å), indicating the double-bond character in the last ones.

BT ligands bridge Cu1 and Cu2 sites while the DPS ligands link only Cu2 sites forming a two-dimensional network, as can be seen in Fig. 4, where several closed paths can be identified. Considering Cu1 and Cu2 as nodes of these closed paths and using the program package TOPOS this compound network topology is described as 6,8-connected bi-nodal system with short Schläfli symbols (3^{10} 4^{10} 5^7 6) (3^8 4^6 5) for Cu1 and Cu2, respectively.

This two-dimensional sheet interacts with other parallel sheets through hydrogen bonds between oxygen atoms from water molecules of one sheet and free oxygen atoms from the carboxylate groups of adjacent sheets [O9···O3 = 2.821(4) Å; O9···O8 = 2.750(4) Å; O12···O5 = 2.749(3) Å] giving rise to a three-dimensional arrangement.

3.4. $\{[Zn_2(BT)(DPS)_2]\cdot 6H_2O\}_n$ (**ZnBTDPS**)

Fig. 5 shows the crystal structure of **ZnBTDPS**, in which the Zn^{2+} coordination sphere presents a distorted tetrahedral geometry. Zn centers are coordinated to two oxygen atoms (O1 and O3) from BT ligands carboxylate groups and to two nitrogen atoms (N1 and N2) from DPS ligands. Table S5 exhibits selected bond distances and angles. The Zn–N bond distances are slightly longer than Zn–O ones. Similarly to **CuBTDPS**, the C–O bonds, in which the oxygen atom is not involved in the coordination toward the metal center, (C11–O2, 1.232(5) and C13–O4, 1.232(5) Å) are shorter than the C–O bonds containing the coordinated oxygen atom (C11–O1, 1.280(5) and C13–O3, 1.291(5) Å).

All four carboxylate groups of BT ligands act in a monodentate coordination mode toward the metal centers, connecting four zinc sites, forming rings of fourteen members as can be seen in Fig. 6. DPS ligands also act in a bridging coordination mode connecting the metal centers generating a 2D coordination network. Considering Zn sites as nodes and using program package TOPOS, this net is a 7-connected uninodal system that can be described with short Schläfli symbols (3^6 4^{14} 6).

This 2D sheet (Fig. 7) interacts with adjacent sheets through weak non-classical hydrogen bonding (CH···O) between DPS ligand CH groups of one sheet with carboxylate free oxygen atoms of adjacent sheets resulting in a three-dimensional supramolecular arrangement.

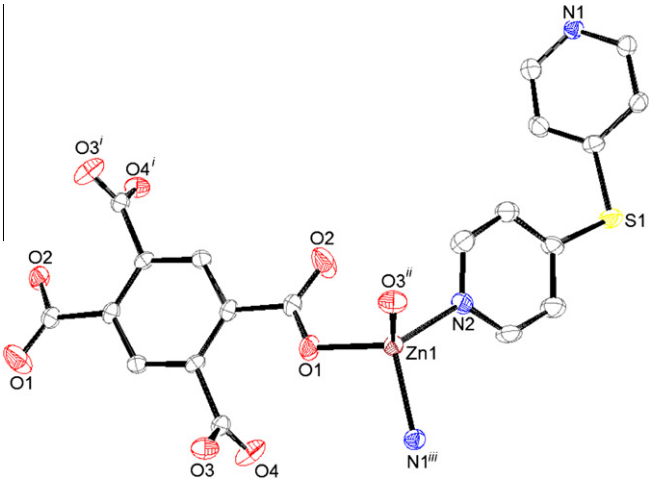

Fig. 5. ORTEP view of structural fragment of compound **ZnBTDPS**. The hydrogen atoms and the lattice water molecules have been omitted for clarity; [symmetry codes: *i*(−*x*, 1 − *y*, 2 − *z*); *ii*(−1 − *x*, 1 − *y*, 2 − *z*) and *iii*(*x*, *y*, 1 + *z*)].

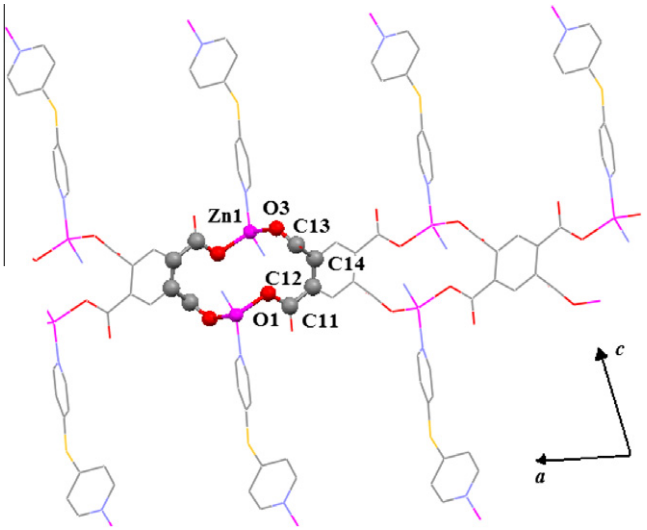

Fig. 6. View along the crystallographic *b*-axis of the 14-members ring formed by Zn centers and BT ligands in **ZnBTDPS** compound. Hydrogen atoms and lattice water molecules were omitted for clarity.

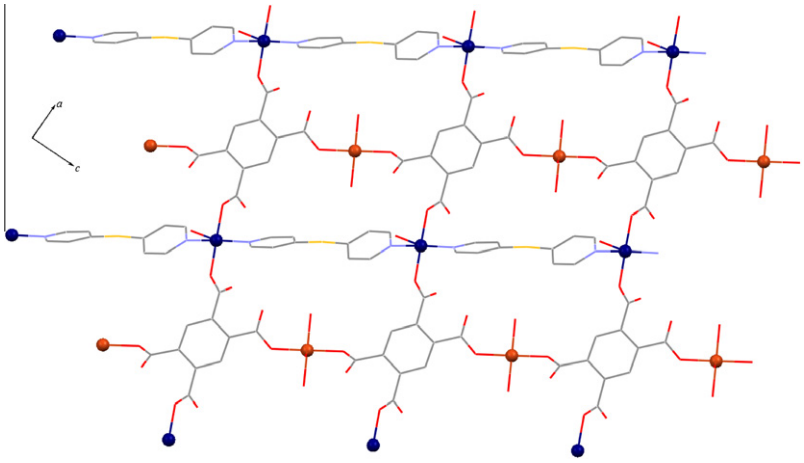

Fig. 4. 2D arrangement of **CuBTDPS** viewed along the crystallographic *b*-axis. The lattice water molecules have been omitted for clarity.

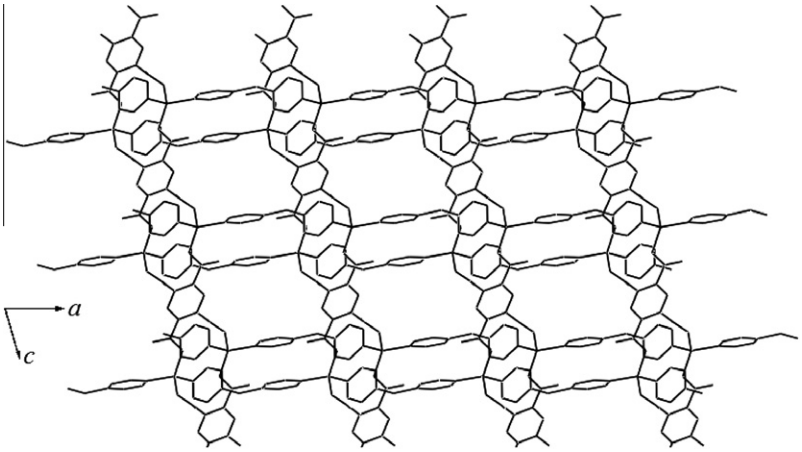

Fig. 7. 2D arrangement of **ZnBTDPS** along crystallographic *b*-axis. The lattice water has been omitted for clarity.

4. Conclusion

The syntheses of four new coordination polymers involving Mn^{2+}, Co^{2+}, Cu^{2+} and Zn^{2+} metal ions and di(4-pyridyl) sulfide (DPS) and 1,2,4,5-benzenetetracarboxylate ion (BT) as ligands are described. All compounds were characterized by means of thermal analysis, vibrational spectroscopy (infrared and Raman) and single crystal X-ray diffraction analysis. In all cases, both BT and DPS ligands are coordinated to metal centers in the bridging mode, giving rise to two-dimensional coordination polymers with different network topologies.

Compounds **MnBTDPS** and **CoBTDPS** are isostructural. The metal sites adopt octahedral geometry, where DPS ligands bridge M1 and M2 sites, while 1,3-carboxylate groups from BT ligands connect M1 sites, generating a 2D rhombohedral sheet. The network can be described as a 4,2-connected bi-nodal system with short Schläfli symbols (6^4 8 10)(6) for M1 and M2, respectively. In compound **CuBTDPS**, both Cu^{2+} sites adopt square-pyramid geometry. BT ligands bridge Cu1 and Cu2 sites through carboxylate groups in a monodentate coordination mode, while the DPS ligands connect Cu2 sites, generating 2D sheets with different closed paths. The system is described as 6,8-connected bi-nodal network of (3^{10} 4^{10} 5^7 6) (3^8 4^6 5) topology for Cu1 and Cu2, respectively. The Zn^{2+} ions adopt tetrahedral geometry in compound **ZnBTDPS**, in which DPS ligand acts in bridging coordination mode and BT ligands connects four zinc atoms, through carboxylate groups in a monodentate coordination mode. These links generate a 7-connected uninodal 2D network of (3^6 4^{14} 6) topology.

Comparing the network topologies of the four compounds, it is noteworthy that Mn^{2+}, Co^{2+} and Cu^{2+} compounds form bi-nodal systems, while Zn^{2+} compound is uninodal. This fact can be explained by the presence of two crystallographically independent metal sites in the asymmetric unit of the first three compounds. It is also interesting to note that only Mn^{2+} and Co^{2+} compounds are isostructural, although the same ligands, stoichiometric ratio and synthesis conditions have been used in all cases. This can be explained by the metals preferred geometry, which in the case of manganese and cobalt is octahedral, while for copper and zinc is square-pyramid and tetrahedral, respectively.

Finally, it has been shown that BT ligand, which has eight oxygen atoms available for coordination toward metal centers or that can act as potential acceptors of hydrogen bonds, is a good candidate to construct supramolecular arrays. As a result of BT ligand presence in all compounds, three-dimensional supramolecular arrangements, driven by hydrogen bondings that clearly control the system crystal packing, were achieved.

Acknowledgments

The authors thank the Brazilian agencies CNPq, CAPES and FAPEMIG (EDT 390/09, APQ-1861-5.02/07) for financial support, and also R.G. Bastos (LDRX-IF/UFF) for the X-ray diffraction facilities.

Appendix A. Supplementary material

CCDC 784981–784984 contains the supplementary crystallographic data for this paper. These data can be obtained free of charge from The Cambridge Crystallographic Data Centre via www.ccdc.cam.ac.uk/data_request/cif.

Supplementary data associated with this article can be found, in the online version, at doi:10.1016/j.ica.2010.12.034.

References

[1] A.J. Blake, N.R. Champness, P. Hubberstey, W.-S. Li, M.A. Withersby, M. Schröder, Coord. Chem. Rev. 183 (1999) 117.
[2] M.V. Marinho, M.I. Yoshida, K. Krambrock, L.F.C. De Oliveira, R. Diniz, F.C. Machado, J. Mol. Struct. 923 (2009) 60.
[3] S.C. Manna, J. Ribas, E. Zangrando, N.R. Chaudhuri, Polyhedron 26 (2007) 4923.
[4] M. Du, S.-T. Chen, X.-H. Bu, J. Ribas, Inorg. Chem. Commun. 5 (2002) 1003.
[5] X.-C. Su, Y.-H. Guo, S.-R. Zhu, H.-K. Lin, J. Mol. Struct. 643 (2002) 147.
[6] Q.-F. Xu, Q.-X. Zhou, J.-M. Lu, X.-W. Xia, L.-H. Wan, Y. Zhang, Polyhedron 26 (2007) 4849.
[7] M.A. Withersby, A.J. Blake, N.R. Champness, P.A. Cooke, P. Hubberstey, W.-S. Li, M. Schro1der, Inorg. Chem. 38 (1999) 2259.
[8] N. Hao, Y. Li, E. Wang, E. Shen, C. Hu, L. Xu, J. Mol. Struct. 697 (2004) 1.
[9] R. Cao, D. Sun, Y. Liang, M. Hong, K. Tatsumi, Q. Shi, Inorg. Chem. 41 (2002) 2087.
[10] Q. Shi, R. Cao, D.-F. Sun, M.-C. Hong, Y.-C. Liang, Polyhedron 20 (2001) 3287.
[11] Y. Li, H. Zhang, E. Wang, N. Hao, C. Hu, Y. Yanc, D. Halld, New J. Chem. 26 (2002) 1619.
[12] D.-Q. Chu, J.-Q. Xu, L.-M. Duan, T.-G. Wang, A.-Q. Tang, L. Ye, Eur. J. Inorg. Chem. (2001) 1135.
[13] H. Kumagai, C.J. Kepert, M. Kurmoo, Inorg. Chem. 41 (2002) 3410.
[14] D.P. Cheng, M.A. Khan, R.P. Houser, Cryst. Growth Des. 2 (2002) 415.
[15] J.-Z. Zou, Q. Liu, Z. Xu, X.-Z. You, X.-Y. Huang, Polyhedron 17 (1998) 1863.
[16] F.D. Rochon, G. Massarweh, Inorg. Chim. Acta 304 (2000) 190.
[17] F.-P. Huang, J.-L. Tian, W. Gu, S.-P. Yan, Inorg. Chem. Commun. 13 (2010) 90.
[18] M.J. Plater, M.R.S. Foreman, R.A. Howie, J.M.S. Skakle, A.M.Z. Slawin, Inorg. Chim. Acta 315 (2001) 126.
[19] F. Jaber, F. Charbonnier, R. Faure, J. Chem. Crystallogr. 27 (1997) 397.
[20] D.P. Cheng, M.A. Khan, R.P. Houser, Inorg. Chim. Acta 351 (2003) 242.
[21] Y. Li, N. Hao, Y. Lu, E. Wang, Z. Kang, C. Hu, Inorg. Chem. 42 (2003) 3119.
[22] C. Ruiz-Pérez, P. Lorenzo-Luis, M. Hernández-Molina, M.M. Laz, F.S. Delgado, P. Gili, M. Julve, Eur. J. Inorg. Chem. (2004) 3873.
[23] O. Fabelo, J. Pasán, L. Cañadillas-Delgado, F.S. Delgado, F. Lloret, M. Julve, C. Ruiz-Pérez, Inorg. Chem. 47 (2008) 8053.
[24] N. Zhang, M.-X. Li, Z.-X. Wanga, M. Shao, S.-R. Zhu, Inorg. Chim. Acta 363 (2010) 8.
[25] O. Fabelo, J. Pasán, F. Lloret, M. Julve, C. Ruiz-Pérez, Inorg. Chem. 47 (2008) 3568.

[26] O.-S. Jung, S.H. Park, D.C. Kim, K.M. Kim, Inorg. Chem. 37 (1998) 610.
[27] O.-S. Jung, S.H. Park, C.H. Park, J.K. Park, Chem. Lett. 28 (1999) 923.
[28] M. Kondo, Y. Shimizu, M. Miyazawa, Y. Irie, A. Nakamura, T. Naito, K. Maeda, F. Uchida, T. Nakamoto, A. Inaba, Chem. Lett. 33 (2004) 514.
[29] S. Muthu, Z. Ni, J.J. Vittal, Inorg. Chim. Acta 358 (2005) 595.
[30] Y. Niu, Z. Li, Y. Song, M. Tanga, B. Wua, X. Xin, J. Solid State Chem. 179 (2006) 4003.
[31] Q.-F. Xu, Q.-X. Zhou, J.-M. Lu, X.-W. Xia, L.-H. Wang, Y. Zhang, Polyhedron 26 (2007) 4849.
[32] G.-H. Zhao, X.-S. Hu, P. Yu, H. Lin, Trans. Met. Chem. 29 (2004) 607.
[33] C. Chachaty, G.C. Pappalardo, G. Scarlata, J. Chem. Soc. Perkin II (1976) 1234.
[34] COLLECT, Enraf-Nonius, Nonius BV, Delft, The Netherlands, 1997, p. 2000.
[35] A.J.M. Duisenberg, J. Appl. Crystallogr. 25 (1992) 92.
[36] A.J.M. Duisenberg, L.M.J. Kroon-Batenburg, A.M.M. Schreurs, J. Appl. Crystallogr. 36 (2003) 220.
[37] G.M. Sheldrick, SHELXL-97 – A Program for Crystal Structure Refinement, 97-2, University of Goettingen, Germany, 1997.
[38] A.C. Larson, Crystallogr. Compd. (1970) 291.
[39] R.H. Blessing, Acta Crystallogr. A51 (1995) 33.
[40] L.J. Farrugia, J. Appl. Crystallogr. 30 (1997) 565.
[41] C.F. Macrae, P.R. Edgington, P. McCabe, E. Pidcock, G.P. Shields, R. Taylor, M. Towler, J. van de Streek, J. Appl. Crystallogr. 39 (2006) 453.
[42] W.M. Teles, N.G. Fernandes, A. Abras, C.A.L. Filgueiras, Trans. Met. Chem. 24 (1999) 321.
[43] R. Scopelliti, G. Bruno, C. Donato, G. Tresoldi, Inorg. Chim. Acta 313 (2001) 43.
[44] M.V. Marinho, M.I. Yoshida, K.J. Guedes, K. Krambrock, A.J. Bortoluzzi, M. Hörner, F.C. Machado, W.M. Teles, Inorg. Chem. 43 (2004) 1539.
[45] D.M. de Faria, M.I. Yoshida, C.B. Pinheiro, K.J. Guedes, K. Krambrock, R. Diniz, L.F.C. de Oliveira, F.C. Machado, Polyhedron 26 (2007) 4525.
[46] R.A. Farani, W.M. Teles, C.B. Pinheiro, K.J. Guedes, K. Krambrock, L.F.C. de Oliveira, F.C. Machado, Inorg. Chim. Acta 361 (2008) 2045.
[47] C.C. Corrêa, R. Diniz, L.H. Chagas, B.L. Rodrigues, M.I. Yoshida, W.M. Teles, F.C. Machado, L.F.C. de Oliveira, Polyhedron 26 (2007) 989.
[48] C.C. Corrêa, R. Diniz, L.H. Chagas, B.L. Rodrigues, M.I. Yoshida, W.M. Teles, F.C. Machado, H.G.M. Edwards, L.F.C. de Oliveira, Vib. Spectrosc. 45 (2007) 82.
[49] G.B. Deacon, R. Phillips, J. Coord. Chem. Rev. 33 (1980) 227.
[50] K. Nakamoto, Infrared and Raman spectra of Inorganic and Coordination Compounds, fourth ed., Wiley, New York, 1986.
[51] V.A. Blatov, Available from: <http://www.topos.ssu.samara.ru/>.
[52] A.W. Addison, T.N. Rao, J. Reedijk, J. Van Rijn, J. Verschoor, J. Chem. Soc., Dalton Trans. (1984) 1349.